Effect of Polymer–Clay Interaction on Solvent Transport Behavior of Fluoroelastomer–Clay Nanocomposites and Prediction of Aspect Ratio of Nanoclay

Madhuchhanda Maiti, Anil K. Bhowmick

Rubber Technology Centre, Indian Institute of Technology, Kharagpur 721302, West Bengal, India

Received 24 August 2006; accepted 27 December 2006
DOI 10.1002/app.26052
Published online 27 March 2007 in Wiley InterScience (www.interscience.wiley.com).

ABSTRACT: Diffusion and sorption of methyl ethyl ketone and tetrahydrofuran through fluoroelastomer-clay nanocomposites were investigated in the temperature range of 30–60°C by swelling experiments. Slightly non-Fickian transport behavior was found for these nanocomposites, having variation of type of nanoclay and loading. Different transport parameters depend on the size and shape of the penetrant molecules. The results were used to study the effect of nanoclay on the solvent transport-properties of nanocomposites and their interactions with solvents. The diffusion coefficient of methyl ethyl ketone at 30°C for neat rubber was 1.43×10^{-8} cm^2 s^{-1}, while those of the unmodified and the modified clay filled samples at 4 phr loading were 0.24×10^{-8} and 0.50×10^{-8} cm^2 s^{-1}, respectively. At 8 and 16 phr loading of the unmodified clay, it was found to be 0.44×10^{-8} and 0.64×10^{-8} cm^2 s^{-1}, respectively. The samples were also reswelled after deswelling. Surprisingly, transport behavior became Fickian on reswelling. Interestingly, ratio of diffusion coefficients of the filled system to the neat system was found to be almost same for the first time swelling and reswelling experiments. The results showed that better polymer-clay interaction in the case of the unmodified-clay filled nanocomposites is responsible for enhanced solvent-resistance property. From the permeation data, for the first time, aspect ratio of nanoclays in different composites was calculated and found to have good correlation with the morphology data obtained from transmission electron microscopy. © 2007 Wiley Periodicals, Inc. J Appl Polym Sci 105: 435–445, 2007

Key words: fluoroelastomers; nanoclays; nanocomposites; solvent transport properties

INTRODUCTION

Polymer-clay nanocomposites possess unique properties because of their nanometer sized features. They can show improved mechanical properties,[1–3] ionic conductivity,[4] flammability resistance,[5] and gas barrier properties[6–8] at low filler loading compared with the conventional microcomposites.

Extensive work on solvent barrier properties has been documented on different rubber-solvent systems.[9–19] However, there are only a few investigations on solvent barrier properties of nanocomposites.[20–24]

It is well known that fluoroelastomers are used in aggressive environments. Stability of the polymeric materials in the presence of aggressive liquid environments is essential for their successful application. So, it is worth investigating to study the barrier properties of the fluoroelastomer-based nanocomposites. In our earlier work, structure–property relationship of these nanocomposites has been reported.[25,26] The liquid environments can be broadly categorized into two types: solvents and nonsolvents. The solvents solvate the elastomers and impart extensive swelling, sometimes leading to degradation, while the nonsolvents without any stresses do not affect the elastomers. The present work deals with the former type.

In this paper, we will focus on the transport properties (i.e., sorption, diffusion and permeation) of different nanocomposites based on fluoroelastomer-nanoclays. The main objective is to investigate the influence of the inorganic filler content and the resultant morphology of the nanocomposites on the sorption and diffusion of two solvents, namely methyl ethyl ketone and tetrahydrofuran. The transport parameters have been calculated for each nanocomposite-solvent system from the conventional weight gain experiment. This single experiment helps to determine simultaneously the diffusion and sorption coefficients of the solvents in the nanocomposite systems. A study of the temperature dependence of these coefficients has been used to calculate the activation parameters and heat of sorption. A reswelling study has been performed also for the first time. The results have been used to predict the extent of nanocomposite–solvent interactions. From the permeability values, the average aspect ratio of nanoclays has been calculated and these values are correlated with transmission electron microscopy data for the first time.

Correspondence to: A. K. Bhowmick (anilkb@rtc.iitkgp.ernet.in).

Journal of Applied Polymer Science, Vol. 105, 435–445 (2007)

TABLE I
Different Formulations for Rubber-Clay Nanocomposites and Their Designation

Composition	Designation	Crosslink density $\times 10^{-4}$, mol/cm^3	Young's modulus, MPa
Viton B-50 + 3 phr DIAK #1	F	57	4.35
Viton B-50 + 4 phr Cloisite NA+ + 3phr DIAK #1	FN4	81	6.17
Viton B-50 + 4 phr Cloisite 20A + 3phr DIAK #1	F20A4	74	5.45
Viton B-50 + 8 phr Cloisite NA+ + 3phr DIAK #1	FN8	82	6.45
Viton B-50 +16 phr Cloisite NA+ + 3phr DIAK #1	FN16	70	6.94

Although microscopy can reveal size and distribution of nanoclay in the rubber matrix, the present experiment may give an idea about the overall average values, which are important for predicting properties. It is also well known that the electron microscopy can only analyze a small surface area at a time and is very tedious.

EXPERIMENTAL

Materials

Viton B-50 (a terpolymer of vinylidene fluoride (VF2), hexafluoropropylene (HFP) and tetrafluoroethylene (TFE), density 1850 kg m^{-3} at 25°C, 68% F, Mooney Viscosity, ML 1 + 10 at 120°C = 39, solubility parameter, $\partial = 14.8 MPa^{1/2}$) was procured from DuPont Dow Elastomers (Freeport, Texas). Nanoclays — Cloisite NA+ (N) and Cloisite 20A (20A) [Surface area = 750 m^2 g^{-1}, layer thickness = 1 nm, aspect ratio = 50–200, initial particles consist of about 6000 platelets, dry particle size = 10% less than 2 μm, 50% less than 6 μm and 90% less than 13 μm (www.nanoclay.com)] were obtained from Southern Clay Products (Texas). Methyl ethyl ketone (MEK) [solubility parameter, $\partial = 19.8 MPa^{1/2}$] was supplied by Nice Chemicals (Cochin, India). Tetrahydrofuran (THF), [solubility parameter, $\partial = 18.6 MPa^{1/2}$] was obtained from S. D. Fine Chem. (Mumbai, India). Hexamethylene diamine carbamate (HMDC, DIAK no. 1) as a crosslinking agent was supplied by NICCO Corp. (Shyamnagar, India).

Preparation of rubber–clay nanocomposites

The rubber was first dissolved in methyl ethyl ketone (20 wt % solution). HMDC dispersion (1 g dispersed in 20 cm^3 methyl ethyl ketone) was then mixed with the rubber solution in a proper proportion to make it 3 phr (parts per 100 g of rubber). The clay, dispersed in methyl ethyl ketone (1 g in 20 cm^3 methyl ethyl ketone) was added to the rubber solution and thoroughly stirred to make a homogeneous mixture, which was then kept in air to evaporate the solvent at room temperature. The samples were then cured at 160°C for 8 min in a hydraulic press.

Table I reports various compositions used for this investigation and their designation. Young's modulus and chemical crosslink density are also given in the table for characterization purpose.

Measurement of transport properties

Sorption experiments were performed by placing the previously weighed test samples into the respective liquid containers (gram of sample versus volume of liquid 1 : 100) maintained at the desired temperature in an oven (S.C. Dey and Co., Kolkata, India). Both MEK and THF, which were used as the solvent, have same molecular weight (72.11), but different structures and solubility parameters. At periodic intervals, the test samples were removed from the liquid containers and the extra solvent on the surface was wiped out quickly with blotting paper and the samples were weighed immediately. After weighing, the samples were placed back into the original test bottles. The experiments were performed at 30, 45, and 60°C.

After equilibrium swelling, the samples were deswollen. For deswelling, the swollen samples were kept in air until these reached a constant weight. It took around 6 h to evaporate off the absorbed solvent completely at 30°C. Then, the whole experiment was also repeated with the deswollen samples at the above-mentioned temperatures.

Transmission electron microscopy

The nanocomposites samples for TEM analysis were prepared by ultra cryomicrotomy using Leica Ultracut UCT. Freshly sharpened glass knives with cutting edge of 45° were used to get the cryosections of 50-nm thickness. Since these samples were elastomeric in nature, the sample temperature during ultra

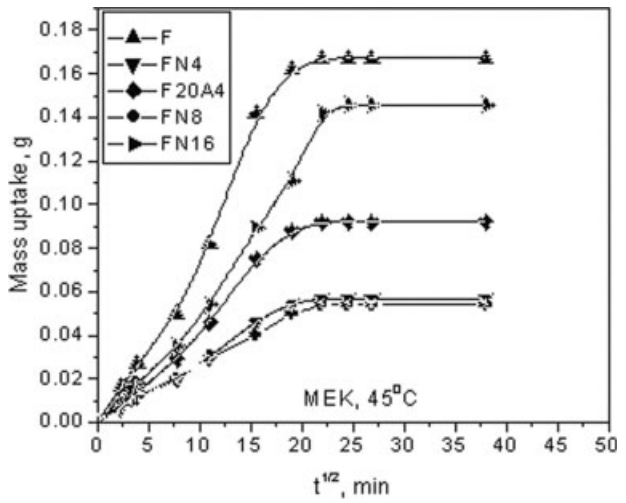

Figure 1 Sorption curves for different nanocomposites at 45°C (solvent MEK).

cryomicrotomy was kept constant at −60°C (which was well below the glass transition temperature, [T_g] of the rubber), at which the samples existed in hard glassy state, thus facilitating ultra cryomicrotomy. The cryosections were collected and directly supported on a copper grid of 200-mesh size. The microscopy was performed later using JEOL-2010 electron microscope (not attached to the cryomicrotomy unit), operating at an accelerating voltage of 200 kV.

The particle length, width and aspect ratio were determined using the image processing software ''UTHSCSA Image Tool.'' For a particular sample several micrographs were analyzed and the average data are reported here.

X-ray dot-mapping

X-ray mapping of the nanocomposites was also performed in an Oxford EDAX system attached to the Scanning Electron microscope (JEOL JSM-800).

X-ray diffraction studies

For the characterization of the rubber nanocomposites, XRD studies were performed using a PHILIPS X-PERT PRO diffractometer in the range of 2–9° and Cu-target ($\lambda = 0.154$ nm). Then, *d*-spacing of the clay particles was calculated using the Bragg's law. The samples were placed vertically in front of the X-ray source. The detector was moving at an angle of 2θ, while the sample was moving at an angle of θ.

Determination of chemical crosslink density and Young's modulus

Chemical crosslink density of the nanocomposites was measured using the well-known Flory-Rehner equation at 25°C:

$$\mu = \frac{-[\ln(1 - V_2) + V_2 + \chi_1 V_2^2]}{V_1[V_2^{1/3} - (V_2/2)]} \quad (1)$$

where, V_2 is the volume fraction of rubber in the swollen gel.

V_1 is the molar volume of the solvent.

χ_1 is the interaction parameter of the rubber with the solvent and was taken as 1 for fluoroelastomer and MEK system at 25°C.[27,28]

Young's modulus of the nanocomposites was calculated from the linear portion of tensile stress-strain curve obtained from Zwick 1445 Universal testing machine at a test rate of 500 mm/min at 25°C.

RESULTS AND DISCUSSION

Sorption

Representative sorption-plots (i.e., mass uptake versus square root of time, $t^{1/2}$) at 45°C for all the nanocomposite-systems are given in Figure 1. All the curves show initially a slightly sigmoidal increase, and later tend to level off. The plateau regions of these curves give the maximum sorption values, M_∞ and the values are tabulated in Table II. Similar plots have been obtained at other temperatures also (not shown here). In this context, it is worth mentioning that the nature of the curves also remains same, if mol % versus $t^{1/2}$ is plotted. It is observed that both these plots (mass uptake versus $t^{1/2}$ and mol % versus $t^{1/2}$) have been used by various workers in the literature.[10,13,29–31] In the present study, mass uptake versus $t^{1/2}$ plots have been used for various calculations (although we have made the mol % plots to arrive at similar conclusions).

The transport mechanism has slight deviation from Fickian mode, as the sorption curves are slightly sigmoidal. To achieve a further insight into the transport mechanism, the sorption results were fitted to the expression

TABLE II
Equilibrium Sorption Values of Different Nanocomposite-Solvent Systems

	M_∞, g					
	MEK			THF		
Sample	30°C	45°C	60°C	30°C	45°C	60°C
F	0.144	0.167	0.181	0.168	0.188	0.206
FN4	0.051	0.057	0.065	0.080	0.086	0.090
F20A4	0.082	0.092	0.117	0.124	0.137	0.148
FN8	0.046	0.054	0.058	0.050	0.071	0.080
FN16	0.095	0.146	0.161	0.130	0.150	0.170

TABLE III
Analysis of Sorption Results of Different Nanocomposite-Solvent Systems

	n					
	MEK			THF		
Sample	30°C	45°C	60°C	30°C	45°C	60°C
F	0.54	0.51	0.46	0.51	0.52	0.49
FN4	0.59	0.43	0.45	0.60	0.58	0.48
F20A4	0.59	0.51	0.49	0.55	0.54	0.54
FN8	0.58	0.43	0.48	0.51	0.48	0.58
FN16	0.58	0.50	0.47	0.54	0.49	0.48

$$\frac{M_t}{M_\infty} = kt^n \tag{2}$$

where M_t is the mass uptake at time t and M_∞ represents the saturated mass uptake at equilibrium, k is a constant which is a characteristic of the system. A value of $n = 0.50$ implies Fickian diffusion. Values of n in the range of $0.50 < n < 1.00$ are indicative of anomalous transport behavior.[10] It is usually assumed that this equation is only valid for short-time (i.e., when $M_t/M_\infty < 0.50$). The n values for different systems at various temperatures are reported in Table III. Most of the systems show slight deviation of $n$value from 0.50. These indicate slightly anomalous transport behavior of these systems including the neat fluorocarbon polymer. Similar behavior is also observed earlier for many polymer systems.[10,32,33] During swelling the shear force experienced by the polymer desorbs the matrix from the filler surface and opens up small vacuoles.[34] This may cause slow leaching out of the low molecular weight polymer-chains during solvent immersion, causing slightly anomalous behavior. The swelling solvents in which the samples were immersed were analyzed by Fourier Transform infrared spectroscopy and indicated presence of small concentration ($\sim 0.5\%$) of fluorocarbon polymer.

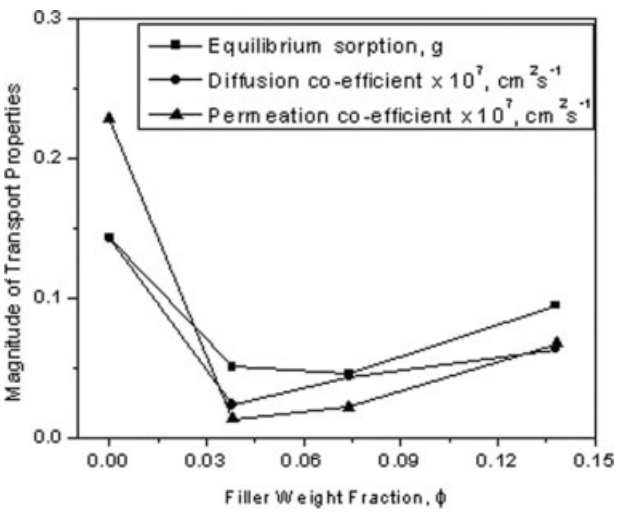

Figure 2 Variation of transport properties with filler loading (solvent MEK) for unmodified clay filled nanocomposites.

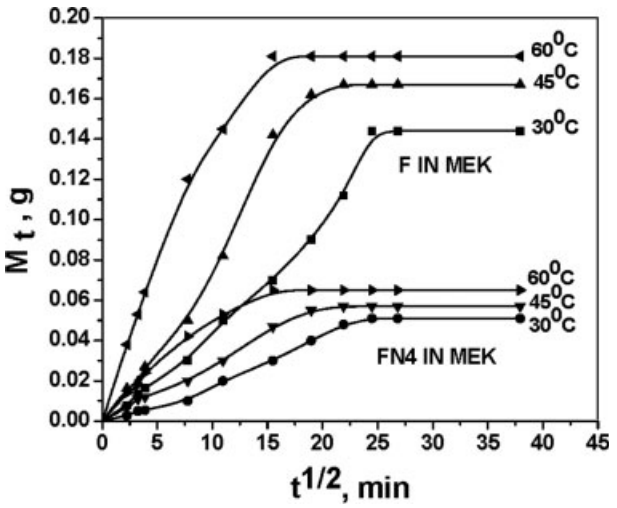

Figure 3 Temperature dependence of sorption curves.

The overall sorption value tends to decrease with the addition of the nanoclays. The decrease is maximum for the unmodified clay filled sample. With filler loading, M_∞ decreases with increasing loading up to 8 phr, beyond which it increases (Fig. 2). As the temperature of swelling increases, the penetrant uptake increases in all the systems (representative curves are shown in Fig. 3). The rate of increase of solvent uptake is slower for the unmodified clay filled sample compared with the modified one. From Table II, it can be seen that the M_∞ values are higher for THF compared with MEK in every composite system. The higher sorption can be explained from the difference in solubility parameter of solvent and rubber ($\partial_s - \partial_r$) and polarity. The solubility parameter value of MEK, THF and the rubber is 19.8, 18.6, and 14.8 $MPa^{1/2}$ respectively. This difference is lower ($3.8 MPa^{1/2}$) in the case of THF than that of MEK ($5.0 MPa^{1/2}$).

Diffusivity

In Figure 4 normalized mass uptake (M_t/M_∞) is plotted against $t^{1/2}/l$ for different nanocomposites, where M_t is the mass uptake at time t (defined as $M_t = (w_t - w_0)/w_0$, where w_t and w_0 are the weight of the sample at time t and the initial weight, respectively. M_∞ represents the saturated mass uptake at equilibrium. For all the samples, the lower slope and nonlinear nature of the M_t/M_∞ values at the initial

stage of the mass uptake followed by a linear behavior with an increased slope was observed from Figure 4. It can be also noticed that the nonlinear region extends up to about $M_t/M_\infty = 0.3$ for all these samples. A similar behavior was observed by other workers.[10,11,35]

The nonlinear behavior of the curves at the initial time may be due to some nonequilibrium phenomena at the early stage of the mass uptake.[35] The initial slower diffusion of the solvent molecules into the nanocomposites may be explained in terms of the fact that the pores at the surface of the dry films are initially closed, and they open up slowly when they are in contact with the solvent. The slope of the linear region of the mass uptake data was used to calculate the diffusion coefficient D of the solvent molecules into the nanocomposite following the literature references.[35,36] For this purpose it was assumed that the simplified Fickian diffusion formula, as given below,

$$\frac{M_t}{M_\infty} = 4\left(\frac{Dt}{\pi l^2}\right)^{1/2} \tag{3}$$

would hold for the linear region of the mass uptake.[19] The use of the Fickian equation to predict the diffusion coefficients quite correctly for non-Fickian diffusions is available in the literature.[10,32,33,35,36] The diffusion coefficient has been calculated for three sets of data separately for all the nanocomposites. The average values are reported in Table IV.

It is found that there is an increase in diffusion coefficient by changing the solvent from MEK to THF for every system. It may be due to the structure of penetrant molecules and the difference in solubility parameters. Diffusivity is dependent on the size and shape of the penetrant molecules.[10] The penetrants have same molecular weight but THF is cyclic

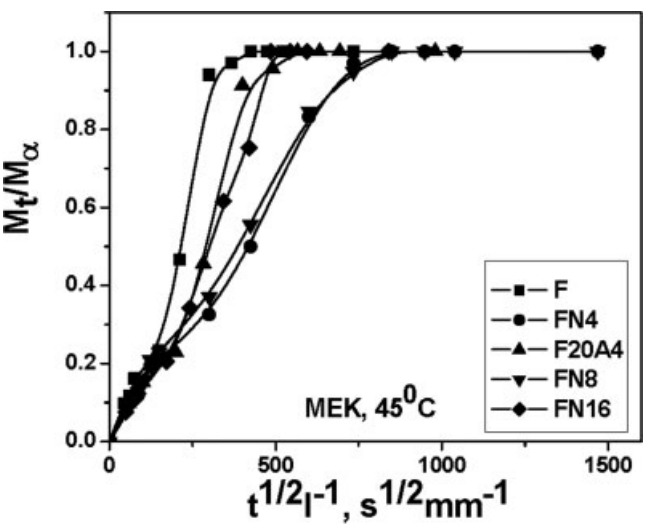

Figure 4 Plot of M_t/M_∞ against $t^{1/2}l^{-1}$.

TABLE IV
Diffusion Coefficients of Different Nanocomposite-Solvent Systems

	Diffusion coefficient, $D \times 10^8$ ($cm^2\ s^{-1}$)					
	MEK			THF		
Sample	30°C	45°C	60°C	30°C	45°C	60°C
F	1.43	3.33	3.50	1.78	3.98	4.52
FN4	0.24	0.59	0.68	0.28	0.64	0.79
F20A4	0.50	0.95	1.13	0.57	1.13	1.33
FN8	0.44	0.87	1.04	0.50	1.04	1.23
FN16	0.64	1.23	1.32	0.71	1.43	1.65

whereas MEK is linear; hence the size of MEK is larger than THF. Therefore, for each nanocomposite, the D value increases with cyclic THF molecules. Also, the difference in solubility parameters of THF and fluoroelastomer is lower than the other system. This may be the other reason for higher diffusion coefficient of THF.

The highest D value is observed in the case of F. The lowest value is registered for FN4 system followed by FN8, F20A4, and FN16. Hence, with the addition of small amount of nanofiller, the diffusion decreases. The nanofillers may form maze-like structure, creating obstacles in the solvent's pathway as shown in Figure 5. Absence of any filler causes F to register the highest D value. When filler is added to the polymer system, it forms a heterogeneous system, where the polymer comprises the continuous phase.[37] Diffusion depends on

(a) the geometry of the dispersed phase (shape, size and size distribution, concentration, concentration distribution and orientation);
(b) properties of the dispersed phase;
(c) properties of the continuous phase and
(d) interaction between the polymer and the nanofiller.

Now, FN4 shows lower D value than FN8. At 4 phr loading, the clay particles are exfoliated as evident from the absence of any peak in the

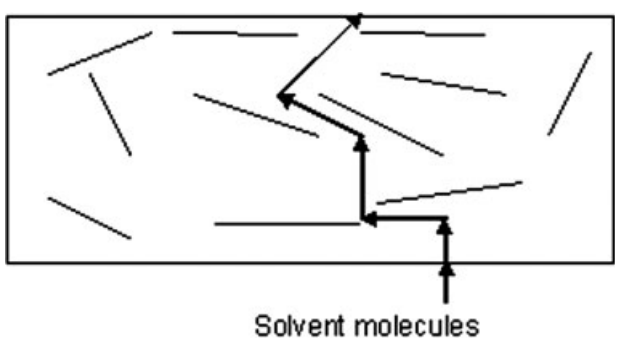

Figure 5 Model showing the tortuous path of the solvent through the nanocomposite.

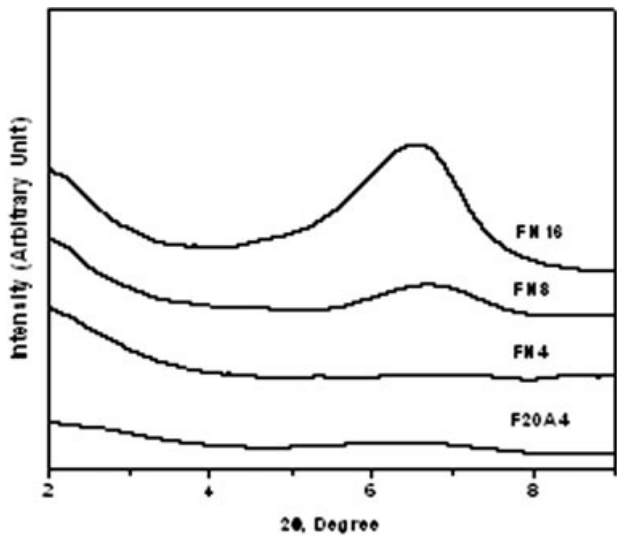

Figure 6 XRD diagrams of different nanocomposites.

XRD diagram (Fig. 6). However, TEM micrograph [Fig. 7(a)] displays mostly exfoliated particles along with some intercalated structures. The X-ray dot mapping also shows homogeneous dispersion of unmodified clay at 4 phr loading [Fig. 7(b)]. But there is a small broad hump in X-ray diffraction of 8 phr filled sample, indicating some ordered structure in the clay layers. It is also evident from the TEM image [Fig. 7(c)], where some agglomeration can be observed along with combination of exfoliation and intercalation. As the clay particles are mostly exfoliated in FN4, they are present as randomly scattered obstacles, producing largest diffusion pathway for this system compared with the others.

On comparing the effect of different types of nanoclay, it is observed that the unmodified clay filled sample registers lower D value as compared with the modified clay filled sample at the same filler loading. This may be due to the presence of mostly exfoliated-intercalated morphology [Fig. 7(d)] in modified clay filled system. Another reason for higher D value in the case of F20A4 may be explained in terms of polymer-filler interaction. As the unmodified clay is more compatible with the polar fluoroelastomer, the interaction with the matrix is much higher.[25] Again the availability of voids larger than the penetrant size increases D value.[10] The better interaction reduces the availability of the voids in the matrix, consequently the diffusivity decreases.

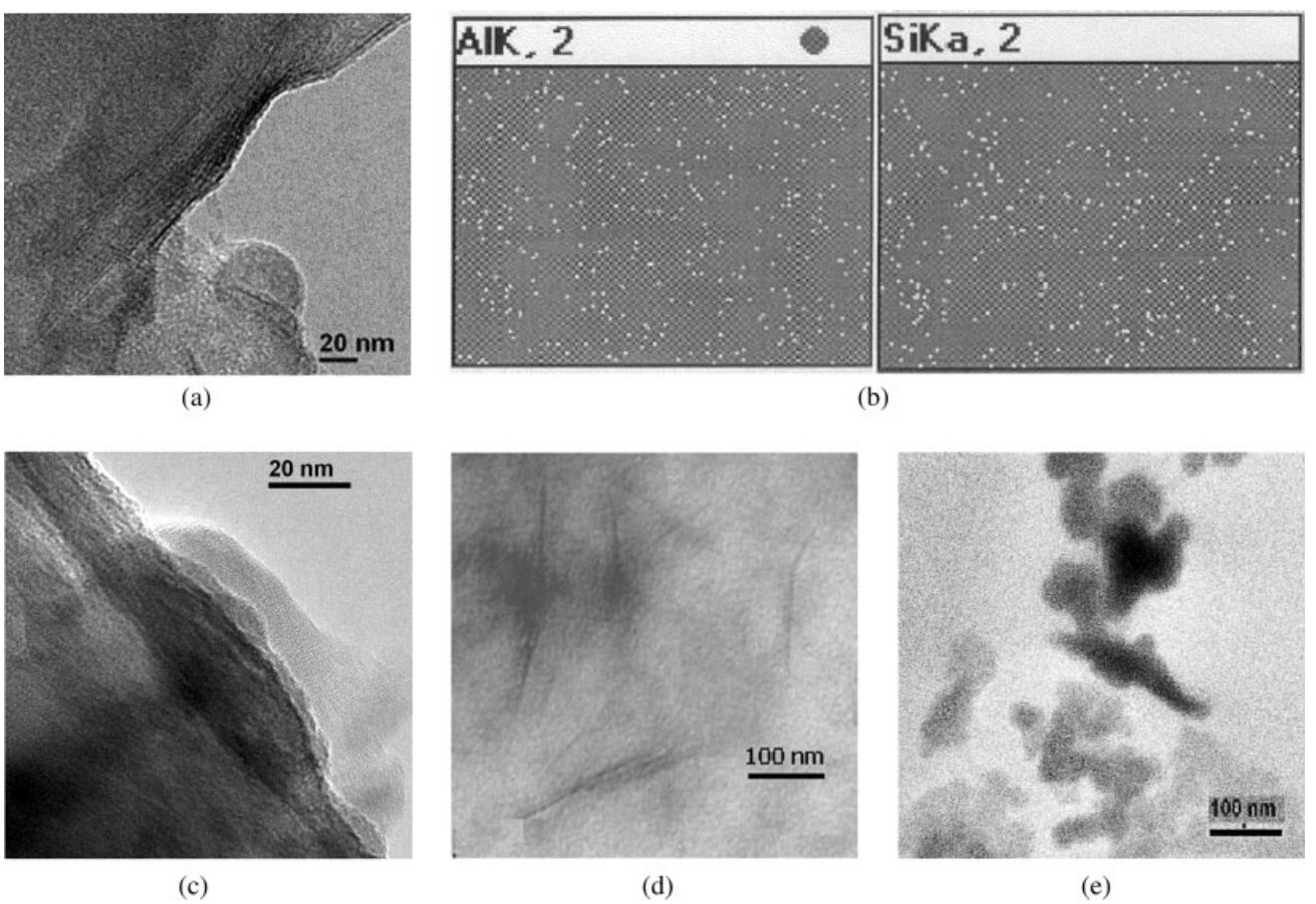

Figure 7 (a) TEM photograph of FN4. (b) X-ray dot mapping of FN4 showing the dispersion of nanoclay (X 200). (c) TEM photograph of FN8. (d) TEM photograph of F20A4. (e) TEM photograph of FN16.

This enhanced interaction restricts the segmental motion of the polymer chains and decreases the size of free volume, and hence availability of voids is less.[38] Higher degree of filler-matrix interaction makes the physical bonds at the interface to withstand the shear force caused by the swelling of the matrix.[34] These are also reflected in the higher value of crosslink density (Table I) and lower sorption value in the case of FN4 as compared with F20A4.

In the case of FN16, the nanoclays tend to agglomerate at high filler loading, [as evident from the peak at 6.6° in the XRD diagram shown in Fig. 6 and the TEM micrograph shown in Fig. 7(e)]. Hence, the interaction with the polymer is less and also the number of obstacles decreases. Decreased solvent's pathway and higher amount of voids help in increasing the D value compared with the other filled systems.

With increasing temperature, D value increases for all the systems. It may be due to the greater segmental motion of the elastomer chains at higher temperature which results in increase in size of free volume and subsequently the D values. Similar results were reported earlier.[10,19]

Permeability and thermodynamic parameters

The mechanism by which small molecules permeate through rubbery polymers involves solution-diffusion process.[37] The permeability coefficient, P, is the product of the diffusion coefficient D and solubility coefficient S:

$$P = DS \tag{4}$$

The P values are reported in Table V. With the addition of low amount of nanofillers (4 phr), permeability decreases tremendously. Least permeability can be observed for FN4 system, followed by FN8, F20A4, and FN16. Here, the values of S are calculated as gram of the liquid sorbed per gram of the nanocomposite. Permeability is in the same line as that of diffusivity. The effect of filler loading on permeability can be clearly visualized from Figure 2.

TABLE V
Permeation Coefficients of Different Nanocomposite-Solvent Systems

	Permeation coefficient, $P \times 10^8$ ($cm^2\ s^{-1}$)					
	MEK			THF		
Sample	30°C	45°C	60°C	30°C	45°C	60°C
F	2.29	6.25	7.12	3.32	8.31	10.35
FN4	0.14	0.37	0.63	0.25	0.62	0.79
F20A4	0.46	0.97	1.49	0.79	1.74	2.19
FN8	0.22	0.52	0.67	0.28	0.82	1.09
FN16	0.68	2.00	2.39	1.03	2.38	3.12

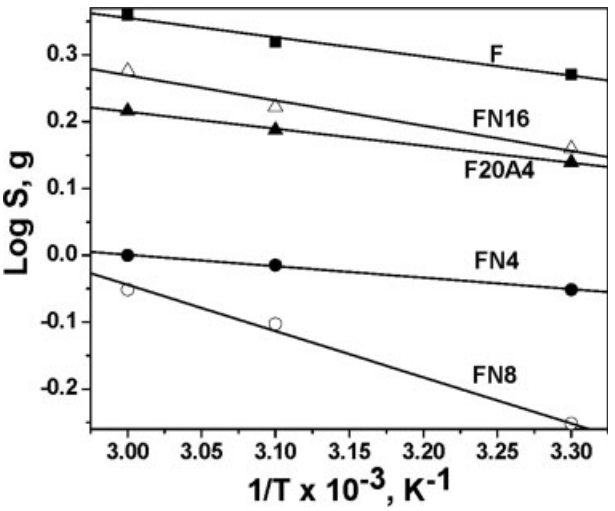

Figure 8 Plot of log S versus temperature for different nanocomposites (solvent THF).

Over a reasonable temperature range, the apparent solubility coefficient can be expressed in terms of a van't Hoff relationship.[10] Using this relationship it is possible to calculate the enthalpy i.e., the heat of sorption, ΔH and entropy, ΔS of a particular composite-solvent system as follows

$$\log S = \frac{\Delta S}{2.303R} - \frac{\Delta H}{2.303RT} \tag{5}$$

The slope of the plot of $\log S$ versus $1/T$ gives ΔH and ΔS can be calculated from the intercept (Fig. 8). The free energy change of the sorption process at 30°C was calculated using the following equation:

$$\Delta G = \Delta H - T\Delta S \tag{6}$$

The thermodynamic parameters are reported in Table VI.

It is observed that ΔH values are positive for all the systems, indicating an endothermic process. Now ΔH is a composite parameter involving both the Henry's law and the Langmuir type sorption mechanisms. In the former type, first there is a formation of a site and then diffusion of the solvent species into that site. The formation of a site is an endothermic process. Hence, it is mainly governed by Henry's law.[10]

The negative ΔG values reported in Table VI, indicate that the sorption is favorable for all the systems. Sorption in THF is more favorable than that in MEK. Sorption is less favorable with the addition of nanoclays compared with the control system. Hence, thermodynamical parameters support the experimental results (Table II).

TABLE VI
Thermodynamic Parameters for Nanocomposite-Solvent Systems

Solvent	Parameters	F	FN4	F20A4	FN8	FN16
MEK	ΔH (kJ mol^{-1})	6.65	6.69	9.39	6.46	15.35
	ΔS (kJ K^{-1} mol^{-1})	0.026	0.023	0.033	0.021	0.053
	ΔG (kJ mol^{-1})	−1.10	−0.16	−0.44	−0.20	−0.44
	E_D (kJ mol^{-1})	9.36	29.96	21.64	21.82	21.26
THF	ΔH (kJ mol^{-1})	5.51	3.30	4.86	13.14	7.23
	ΔS (kJ K^{-1} mol^{-1})	0.023	0.012	0.019	0.045	0.027
	ΔG (kJ mol^{-1})	−1.34	−0.28	−0.80	−0.27	−0.82
	E_D (kJ mol^{-1})	8.38	28.95	20.61	20.63	20.39

According to Fick's law, the diffusion coefficient follows an Arrhenius relationship, in the case of diffusion of liquids through the amorphous polymers.

$$D = D_0 e\left(\frac{-E_D}{RT}\right) \tag{7}$$

where, E_D is the activation energy required to create an opening in the matrix to allow the penetrant molecule to pass. Thus, E_D is a function of the inter and intramolecular force of attraction between the elastomer chains, dispersion of the fillers and also the polymer-filler interaction forces that must be overcome to create the space for a unit diffusion process of one mole of the penetrant. Hence, the E_D value will be greater for the larger penetrant molecules, the polymers having stronger cohesive energy, rigid chain and increased polymer-filler interaction. Now in the concerned nanocomposites, as the base polymer is same, only two factors should be considered: (1) penetrant size and (2) polymer-filler interaction.

A representative plot of log D versus temperature is shown in Figure 9. The slope of the curves gives the E_D values. As THF has smaller size, the E_D values are lower compared with MEK in every system (Table VI). Highest E_D value for FN4 may be due to the best polymer-filler interaction. Polar hydroxyl groups of the unmodified clay attract the chains of fluoroelastomers having $C^{\delta+}$-$F^{\delta-}$ bonds. In the case of the modified clays, there may be some incompatibility with the matrix due to modification by long chain amines. The variation in E_D with filler loading can be explained using the same argument applied for change in D, which has been discussed in the earlier section.

Thus, the addition of nanofillers to a neat elastomer, improves the solvent barrier properties mostly due to the combined effect of the following phenomena:

(a) The decrease in area available for diffusion, as a result of impermeable clay layers replacing the permeable elastomer.
(b) The increase in the distance traveled by the solvent to cross the film as it goes through a tortuous path around the clay layers, which can be clearly understood from the model shown in Figure 5.

Reswelling of the samples

A representative sorption curve of the samples obtained from reswelling experiment is shown in Figure 10. Surprisingly, the initial sigmoidal portion, observed for the first time swelling, is absent here. It confirms that the initial sigmoidal portion observed previously is mainly due to the leaching out of the low molecular weight chains of the polymer. The M_∞ values have been reported in Table VII. Mass uptake on reswelling has been increased several times compared with the swelling experiment. The highest M_∞ value is observed for F followed by F20A4 and FN4. The trend is in line with that observed in the case of first time swelling.

In Figure 11, normalized mass uptake (M_t/M_∞) is plotted against $t^{1/2}/l$ for different nanocomposites. The diffusion is Fickian in nature here. The diffusion and permeation coefficients are reported in Table VIII. Both the coefficients are highest in F followed by F20A4 and FN4. The reason for this trend may be

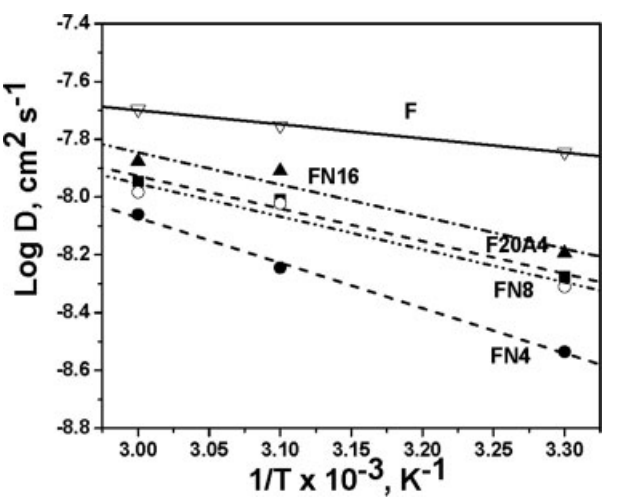

Figure 9 Plot of log D versus temperature for different nanocomposites (solvent MEK).

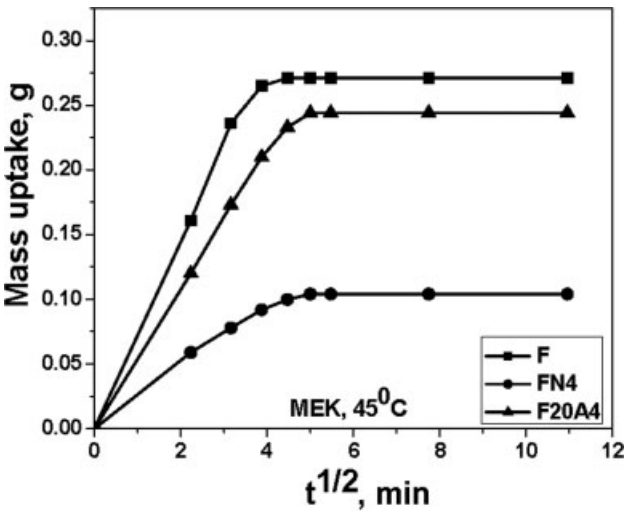

Figure 10 Sorption curves for different nanocomposites obtained from reswelling experiment at 45°C (solvent MEK).

same as explained earlier. But diffusion and consequently the permeation have been increased many folds compared with the first swelling for all the samples. Interestingly, the ratio of diffusion and permeation coefficients of the filled samples to the neat one remains almost same here, when compared with first swelling experiment (Table IX). This proves the solvent cannot destroy the polymer-filler interaction. For reswelling experiment, the path for the solvent may have become well-defined, as some low molecular weight chains may leach out during the first swelling, creating some voids in the systems. Because of this increased free volume, diffusion becomes faster in the reswelling experiment.

Aspect ratio

Addition of layered nanoclays to a neat polymer restricts the permeability, which is a product of diffusibility and solubility, due to the following phenomena:

1. The available area for diffusion will decrease as a result of impermeable nanoclays replacing the permeable polymer. As the area of contact between polymer and solvent decreases, solubility will also decrease.
2. When nanoclays are added to the system, we may assume that the clay layers are randomly placed in the matrix. The diffusion of the solvent will detour around the impermeable clay layers. Diffusion will be diverted to pass a clay platelet in every layer and hence, the solvent must have to travel a longer path (d_f) in the filled system compared with that (d_0) for the neat polymer.

Using scaling concept, permeability P can be written as

$$P \sim A/d \tag{8}$$

where A is the cross-sectional area available for diffusion and d is the path length the solvent must travel to cross the sample.

As a result, the permeability of nanocomposites (P_f) is reduced from that of the neat polymer (P_0) by the product of the decreased area and the increased path length as follows:

$$\frac{P_0}{P_f} = \left(\frac{A_0}{A_f}\right)\left(\frac{d_f}{d_0}\right) \tag{9}$$

where A_0 is the cross-sectional area available for diffusion in a neat polymer sample, A_f the cross-sectional area available for diffusion in a nanocomposite, d_0 is the sample thickness (i.e., the distance a solvent molecule must travel to cross the neat polymer sample), d_f is the distance a solvent molecule must travel to cross the nanocomposite sample.

TABLE VII
Equilibrium Sorption Values of Different Nanocomposite-Solvent Systems (Reswelling)

Sample (after leaching out)	$M\infty$, g					
	MEK			THF		
	30°C	45°C	60°C	30°C	45°C	60°C
F	0.260	0.271	0.281	0.274	0.284	0.294
FN4	0.087	0.104	0.115	0.139	0.153	0.168
F20A4	0.218	0.244	0.253	0.237	0.261	0.271

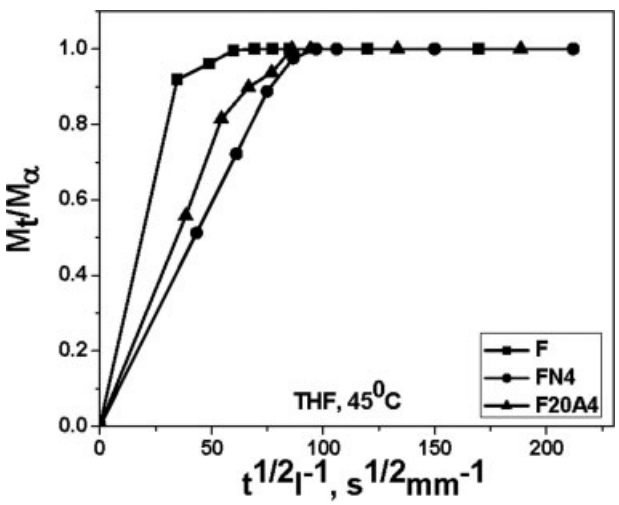

Figure 11 Plot of M_t/M_∞ against $t^{1/2}l^{-1}$ (obtained from reswelling experiment).

TABLE VIII
Diffusion and Permeation Coefficients of Different Nanocomposite-Solvent Systems (Reswelling)

Sample (after leaching out	Diffusion coefficient, $D \times 10^7$ ($cm^2\ s^{-1}$)						Permeation coefficient, $P \times 10^6$ ($cm^2\ s^{-1}$)					
	MEK			THF			MEK			THF		
	30°C	45°C	60°C	30°C	45°C	60°C	30°C	45°C	60°C	30°C	45°C	60°C
F	13.90	20.10	23.00	14.30	20.22	23.70	4.30	6.56	8.28	6.99	10.75	13.11
FN4	2.22	3.68	5.00	3.32	4.42	5.03	0.24	0.42	0.65	0.54	0.77	0.96
F20A4	4.25	5.60	7.60	4.72	6.50	8.25	0.83	1.03	1.52	1.29	1.83	2.53

TABLE IX
Ratio of Diffusion and Permeation Coefficients of Different Nanocomposites to Neat Polymer System Obtained From First Time Swelling and Reswelling Experiments

Sample (after leaching out	D_{filled}/D_{neat}						P_{filled}/P_{neat}					
	MEK			THF			MEK			THF		
	30°C	45°C	60°C	30°C	45°C	60°C	30°C	45°C	60°C	30°C	45°C	60°C
FN4	0.17	0.18	0.19	0.16	0.16	0.17	0.06	0.06	0.09	0.08	0.07	0.08
F20A49	0.35	0.29	0.32	0.32	0.28	0.29	0.20	0.16	0.21	0.24	0.21	0.21
FN4 (reswelled)	0.16	0.18	0.22	0.21	0.21	0.21	0.06	0.06	0.08	0.08	0.07	0.07
F20A4 (reswelled)	0.31	0.28	0.33	0.33	0.31	0.35	0.19	0.16	0.18	0.18	0.17	0.19

Now,

$$\frac{P_0}{P_f} = \frac{\frac{V_0}{d_0}}{\frac{(V_0 - V_f)}{d_f}} \left(\frac{d_f}{d_0}\right) \tag{10}$$

where V_0 is the total volume of the neat polymer sample and V_f is the volume of nanoclays in the nanocomposite-sample.

$$\frac{P_0}{P_f} = \frac{V_0}{V_0 - V_f} \left(\frac{d_f}{d_0}\right)^2 \tag{11}$$

$$= \frac{1}{1-\phi} \left(\frac{d_f}{d_0}\right)^2 \tag{12}$$

where ϕ is the volume fraction of filler.

When a solvent diffuses across a neat polymer, it must travel the thickness of the sample (d_0). When the same solvent diffuses through a nanocomposite film with nanoclays, its path length is increased by the distance it must travel around each clay layer it strikes. According to Lan et al.[39] the path length of a gas molecule diffusing through an exfoliated nanocomposite is

$$d_f = d_0 + \frac{d_0 L \phi}{2 d_c} \tag{13}$$

where L and d_c are the length and thickness of a clay layer respectively.

Substituting this value in eq. (11),

$$\frac{P_0}{P_f} = \frac{1}{1-\phi} \left(1 + \frac{L\phi}{2d_c}\right)^2 \tag{14}$$

$$= \frac{1}{1-\phi} \left(1 + \frac{\alpha\phi}{2}\right)^2 \tag{15}$$

where, aspect ratio, $\frac{L}{d_c} = \alpha$

The aspect ratio of the nanoclays in different samples has been calculated using eq. (15) and is reported in Table X. It may be mentioned that under a variety of experimental conditions (i.e., solvent, temperature, swelling or reswelling) the aspect ratio values are very close for a particular system. In the table, the average of aspect ratios calculated from the permeability data in two different solvents at three different temperatures for swelling and reswelling experiments have been reported. It is observed that the aspect ratio is highest (146 ± 14) in the case of FN4. Similarly, the aspect ratios are 63 ± 5, 60 ± 4 and 10 ± 1 for F20A4, FN8, and FN16, respectively. These values are in good accord with those measured from the transmission electron micrographs (Table X). In Figure 12, average aspect ratios, measured from swelling experiment and morphology have been plotted. There is a linear relationship between the aspect ratios calculated from these two methods with excellent correlation coefficient. It is also interesting to note that the aspect ratio for a particular sample in two different solvent systems at three different temperatures is in the same range, which means that it is independent of the solvent and temperature. The aspect ratios calculated from

TABLE X
Average Aspect Ratio of Clay Layers Present in Different Nanocomposites

Sample	Aspect ratio	
	Swelling	Morphology
FN4	146 ± 14	145 ± 6
F20A4	63 ± 5	53 ± 6
FN8	60 ± 4	60 ± 9
FN16	10 ± 1	6 ± 2

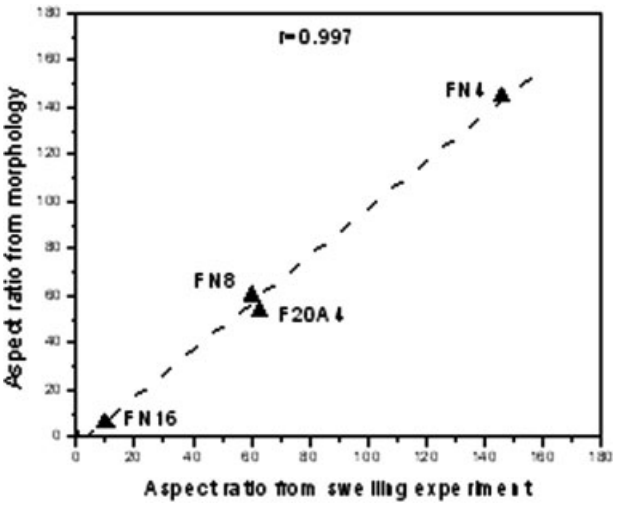

Figure 12 Comparison of aspect ratio from swelling experiment and electron micrographs.

first time swelling and reswelling experiments are also in the same range. This confirms that the model proposed in eq. (15) is in independent of solvent and temperature.

CONCLUSIONS

Solvent transport properties of fluoroelastomer-clay nanocomposites having various types and loadings of nanoclays have been investigated in this work. Permeability decreases significantly with the addition of only 4 phr of the unmodified montmorillonite clay (0.14×10^{-8} cm^2 s^{-1}) compared with that of neat polymer (2.29×10^{-8} cm^2 s^{-1}). The activation energy of diffusion increased tremendously with the addition of nanoclays (35.74 and 27.64 kJ mol^{-1} for the unmodified and the modified clay filled samples respectively) compared with the control system (9.36 kJ mol^{-1}) in the temperature range of 30–60°C. The unmodified clay filled sample shows lower sorption, diffusion, and permeation compared with those of the modified clay filled sample at the same filler loading due to better polymer-filler interaction. With increasing filler loading, overall permeability increases due to the enhanced tendency of clay agglomeration. Temperature has an adverse effect on the solvent transport properties in all the nanocomposites. Surprisingly, in the reswelling experiment, the nature of sorption and diffusion becomes Fickian and the ratio of diffusion coefficients of the filled to the neat system remains almost the same as obtained in first time swelling. Aspect ratio of the nanoclays has been calculated from the permeability data. These are in good accord with the values measured from the transmission electron micrographs.

References

1. Usuki, A.; Kojima, Y.; Okada, A.; Kamigaito, O. J Mater Res 1993, 8, 1185.
2. Lan, T.; Pinnavaia, T. J. Chem Mater 1994, 6, 2216.
3. Sadhu, S.; Bhowmick, A. K. J Polym Sci Part B: Polym Phys 2004, 42, 1573.
4. Vaia, R. A.; Vasudevan, S.; Krawice, W.; Scanlon, L. G.; Giannelis, E. P. Adv Mater 1995, 7, 154.
5. Gilman, J. W. Appl Clay Sci 1999, 15, 31.
6. Tong, X.; Zhaw, H.; Tang, T.; Feng, Z.; Huang, B. J Polym Sci Part A: Polym Chem 2002, 40, 1706.
7. Messermith, P. B.; Giannelis, E. P. J Polym Sci Part A: Polym Chem 1995, 33, 1049.
8. Gorrasia, G.; Tortoraa, M.; Vittoriaa, V.; Polletb, E.; Lepoittevinb, B.; Alexandreb, M.; Dubois, P. Polymer 2003, 44, 2271.
9. Cassidy, P. E.; Aminabhavi, T. M. Rubber Chem Technol 1983, 56, 594.
10. Harogoppad, S. B.; Aminabhavi, T. M. Macromolecules 1991, 24, 2598.
11. Khinnavar, R. D.; Aminabhavi, T. M. J Appl Polym Sci 1991, 42, 2321.
12. Proikakis, C. S.; Mamouzelos, N. J.; Tarantili, P. A.; Andreopoulos, A. G. Polym Degrad Stab 2006, 91, 614.
13. Gopakumar, S.; Gopinathan Nair, M. R. Polymer 2005, 46, 10419.
14. Azaar, K.; Rosca, I. D.; Vergnaud, J. M. Polymer 2002, 43, 4261.
15. Kader, M. A.; Bhowmick, A. K. Polym Degrad Stab 2003, 79, 283.
16. Mathai, A. E.; Singh, R. P.; Thomas, S. J Membr Sci 2002, 202, 35.
17. El-Tantawy, F. Polym Degrad Stab 2001, 73, 289.
18. Erdal, S.; Bahar, I.; Erman, B. Polymer 1998, 39, 2035.
19. Sen Majumder, P.; Majali, A. B.; Tikku, V. K.; Bhowmick, A. K. J Appl Polym Sci 2000, 75, 784.
20. Brunside, S. D.; Giannelis, E. P. Chem Mater 1995, 7, 1597.
21. Jiang, T.; Wang, Y.; Yeh J.; Fan, Z. Eur Polym J 2005, 41, 459.
22. Chen, T.-K.; Tien, Y.-I.; Wei, K.-H. Polymer 2000, 41, 1345.
23. Kim, B. K.; Seo, J. W.; Jeong, H. M. Eur Polym J 2003, 39, 85.
24. Wang, Z.; Pinnavaia, T. J. Chem Mater 1998, 10, 3769.
25. Maiti, M.; Bhowmick, A. K. J Polym Sci Part B: Polym Phys 2006, 44, 162.
26. Maiti, M.; Bhowmick, A. K. J Appl Polym Sci 2006, 101, 2407.
27. Fogiel, A. W. J Polym Sci Polym Symp 1975, 53, 333.
28. Mitra, S.; Ghanbari-Siahkali, A.; Kingshott, P.; Almdal, K.; Kem Rehmeier, H.; Christensen, A. G. Polym Degrad Stab 2004, 83, 195.
29. Gopalan Nair, K.; Dufresne, A. Biomacromolecules 2003, 4, 657.
30. Okay, O.; Durmaz S.; Erman, B.; Macromolecules 2000, 33, 4822.
31. Nandi, S.; Winter, H. H. Macromolecules 2005, 38, 4447.
32. Vogt, B. D.; Soles, C. L.; Lee, H.-J.; Lin, E. K.; Wu, W.-I. Polymer 2005, 46, 1635.
33. Shafee, E. E.; Naguib, H. F. Polymer 2003, 44, 1647.
34. Kraus G., Ed. Reinforcement of Elastomers; Interscience Publishers: New York, 1965; p 147.
35. Singh, A.; Mukherjee, M. Macromolecules 2005, 38, 8795.
36. Vogt, B. D.; Soles, C. L.; Lee, H.-J.; Lin, E. K.; Wu, W.-I. Langmuir 2004, 20, 1453.
37. Crank, J.; Park, G. S., Eds., Diffusion in Polymers; Academic Press: New York, 1968.
38. Lee, W. M. Polym Eng Sci 1980, 20, 1.
39. Lan T.; Kaviratna, P. D.; Pinnavaia, T. J. Chem Mater 1994, 6, 573.